

Converted-wave reflection seismology over inhomogeneous, anisotropic media

Leon Thomsen*

ABSTRACT

Converted-wave processing is more critically dependent on physical assumptions concerning rock velocities than is pure-mode processing, because not only moveout but also the offset of the imaged point itself depend upon the physical parameters of the medium. Hence, unrealistic assumptions of homogeneity and isotropy are more critical than for pure-mode propagation, where the image-point offset is determined geometrically rather than physically. In layered anisotropic media, an effective velocity ratio $\gamma_{eff} \equiv \gamma_2^2/\gamma_0$ (where $\gamma_0 \equiv \bar{V}_p/\bar{V}_s$ is the ratio of average vertical velocities and γ_2 is the corresponding ratio of short-spread moveout velocities) governs most of the behavior of the conversion-point offset. These ratios can be constructed from *P*-wave and converted-wave data if an approximate correlation is established between corresponding reflection events. Acquisition designs based naively on γ_0 instead of γ_{eff} can

result in suboptimal data collection. Computer programs that implement algorithms for isotropic homogeneous media can be forced to treat layered anisotropic media, sometimes with good precision, with the simple provision of γ_{eff} as input for a velocity ratio function. However, simple closed-form expressions permit hyperbolic and posthyperbolic moveout removal and computation of conversion-point offset without these restrictive assumptions. In these equations, vertical traveltimes is preferred (over depth) as an independent variable, since the determination of the depth is imprecise in the presence of polar anisotropy and may be postponed until later in the flow. If the subsurface has lateral variability and/or azimuthal anisotropy, then the converted-wave data are not invariant under the exchange of source and receiver positions; hence, a split-spread gather may have asymmetric moveout. Particularly in 3-D surveys, ignoring this diodic feature of the converted-wave velocity field may lead to imaging errors.

INTRODUCTION

The subject of converted waves is receiving new attention, principally because of the new practicality of multicomponent ocean-bottom seismology (OBS) and the high data quality often achieved in that context. However, processing such data normally relies on classic algorithms such as that of Tessmer and Behle (1988), which is based on the simple model of an isotropic homogeneous layer or on naive extensions of it. This paper extends their work to the minimally realistic case of many layers, which may or may not be anisotropic, and recasts important results of Tsvankin and Thomsen (1994) to make converted-wave processing practicable in realistic situations. It also discusses some elementary features of converted waves in laterally inhomogeneous media.

Any elastic wave incident upon any elastic discontinuity generally converts some of its energy to transmitted and reflected

waves of other types. If the conversion happens once only from an incident *P*-wave to a reflected *S*-wave, we call this mode a *C*-wave. Normally, the determination that an arriving shear wave has converted at the reflector (*C*-mode) rather than at some other horizon is a nontrivial determination, often requiring a good understanding of the velocity structure in the overburden. Such mode determination is outside the scope of this paper, which concerns only the analysis of *C*-waves themselves.

In anisotropic media, each such conversion generally reflects both fast and slow shear waves, whose modes may be termed fast and slow *C*-modes. In this work, we concentrate mostly on flat-lying polar anisotropic (vertical transversely isotropic, or VTI) layers for which only one *C*-mode (polarized in-line) is reflected. However, most results are approximately applicable to data from azimuthally anisotropic media, so long as the difference between fast and slow shear velocities is much

Manuscript received by the Editor December 4, 1997; revised manuscript received October 13, 1998.

*BP Amoco Production Co., 501 Westlake Park Blvd., Houston, Texas 77079. E-mail: lthomsen@amoco.com.

© 1999 Society of Exploration Geophysicists. All rights reserved.

smaller than the difference between these and the *P*-wave velocity; this condition is commonly satisfied.

Many of the principal difficulties in *C*-wave exploration are implicit in Figure 1, which shows a thick, uniform isotropic layer. A ray emitted as a *P*-wave at angle θ_p from the surface source at *S* reflects from the bottom of the layer as an *S*-wave at angle θ_s and is received at *x*. The two angles are related by Snell's law:

$$\sin \theta_p / V_p = \sin \theta_s / V_s = p = \frac{\partial t_c}{\partial x}, \quad (1)$$

where *p* is the ray parameter (constant along the ray) and t_c is the arrival time of the *C*-wave at offset *x*. Note that the offset x_c to the image point at depth in the subsurface (illuminated by this ray) differs from the midpoint by a distance that depends upon a physical parameter, i.e., the ratio $\gamma = V_p / V_s$ in the overburden (Tessmer and Behle, 1988). By contrast, in pure-mode propagation through this geometry, the offset to the illuminated point ($x/2$) is determined geometrically, and no physical parameter need be determined. This remains true even if the subsurface is vertically inhomogeneous (layered) or polar anisotropic. This difference causes fundamental differences in processing strategy and tactics.

Because γ is a physical parameter, its value depends on physical assumptions, e.g., those of vertical homogeneity and/or isotropy. Hence, physical properties play a larger role in the analysis of *C*-waves, and the inhomogeneity and anisotropy of the medium are much more crucial than for *P*-waves. One cannot form a proper image of the subsurface without careful consideration of this physical parameter, whereas in pure mode propagation, physical characterization may follow imaging.

Because $\gamma > 1$, the *S*-wave leg comes up more steeply than the *P*-wave leg goes down. Since this *C*-wave arrival is polarized transversely, a horizontally polarized receiver is better suited for detecting it than a vertically polarized receiver. (In this isotropic, flat-lying geometry, the energy appears only on the vertical and in-line horizontal components. More interesting cases are considered in the following.)

We first give a reformulation and discussion of the equations of Tessmer and Behle (1988) and Tsvankin and Thomsen (1994) for the isotropic, homogeneous case to establish a base for understanding more realistic cases.

ARRIVAL TIMES AND VELOCITIES: HOMOGENEOUS AND ISOTROPIC

Even in the single uniform isotropic layer of Figure 1, the moveout of the *C*-wave is not hyperbolic. In this simple case, the exact traveltime is given (through elementary tri-

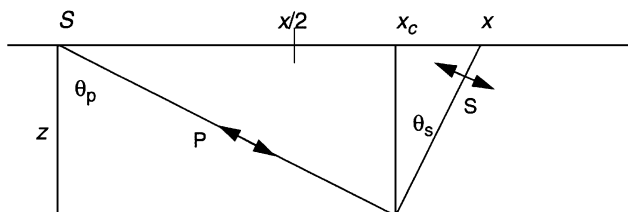


FIG. 1. Canonical converted-wave schematic.

gonometry) as

$$t_c(x) = t_p(x) + t_s(x) = \frac{z}{V_p \cos \theta_p(x)} + \frac{z}{V_s \cos \theta_s(x)}, \quad (2)$$

where t_p is the one-way oblique traveltime through the layer for the *P*-wave and t_s is the corresponding one-way shear time. Similarly, the exact emergence offset *x* is given by

$$x = V_p t_p \sin \theta_p + V_s t_s \sin \theta_s = p V_p^2 t_p + p V_s^2 t_s. \quad (3)$$

However, for more complicated cases (to be considered later), we will need approximations. Here we expand these exact expressions as a Taylor series in t^2 versus x^2 (see Tsvankin and Thomsen, 1994):

$$t_c^2(x) = t_{c0}^2 + x^2 / V_{c2}^2 + A_4 x^4 + \dots \quad (4)$$

Let us consider these terms in order. The two-way *C*-wave zero-offset time t_{c0} , which corresponds to vertical travel in this context, may be written in terms of the one-way pure-mode times as

$$t_{c0} = t_{p0} + t_{s0} = t_{p0}(1 + t_{s0}/t_{p0}) = t_{p0}(1 + \gamma) \quad (5)$$

since

$$\gamma \equiv V_p / V_s = \frac{z/t_{p0}}{z/t_{s0}} = t_{s0}/t_{p0},$$

with the unknown depth *z* cancelling out. In the present context, the amplitude of the energy arriving at vertical incidence is zero (Aki and Richards, 1980), but the time t_{c0} may still be found by extrapolating times from obliquely incident arrivals to zero offset or by examining *C*-wave stacks. Of course, the determination of t_{p0} requires separate *P*-wave data and an interpreted correspondence between *P*-wave and *C*-wave arrivals. We assume this is available.

The *C*-wave short-spread moveout velocity V_{c2} in equation (4) is given (see the Appendix) by

$$V_{c2}^2 = \frac{V_p^2 t_{p0} + V_s^2 t_{s0}}{t_{p0} + t_{s0}} = \frac{V_p^2}{1 + \gamma} + \frac{V_s^2}{1 + 1/\gamma} \quad (6)$$

{In the simple case of Figure 1, this velocity simplifies to

$$V_{c2}^2 = V_p V_s = \sqrt{V_{p2}^2 V_{s2}^2} = V_{p2}^2 / \gamma. \quad (7)$$

However, this is not true in the more realistic cases to be considered shortly, so we do not use it here.}

The quartic moveout parameter A_4 of equation (4) was derived by Tsvankin and Thomsen (1994) and is discussed further in the Appendix. For the single homogeneous isotropic layer of Figure 1, it is given by

$$A_4 = \frac{-(\gamma - 1)^2}{4(\gamma + 1)t_{c0}^2 V_{c2}^4}. \quad (8)$$

This means that, for a typical target at $x/z = 1$, the quartic term is -25% of the hyperbolic term if $\gamma = 3$ or -8% if $\gamma = 2$. It also means that A_4 is not independent of the previously determined parameters (γ, V_{c2}) and is not available for fitting, e.g., to flatten the gathers. (We obtain a free parameter A_4 in the following sections.)

This completes the discussion of the Taylor series expansion [equation (4)] for the *C*-wave travel time, except to note that it is not a very good approximation. In the limit of large *x*, it

implies that t^2 should be increasing as x^4 , which is obviously not reasonable; instead, it should be increasing as x^2 , but with the correct velocity coefficient. Tsvankin and Thomsen (1994) show, in the pure-mode context, how to approximate this behavior by modifying the quartic term. Using the same idea here, equation (4) is replaced by

$$t_c^2(x) = t_{c0}^2 + x^2/V_{c2}^2 + \frac{A_4 x^4}{1 + A_5 x^2}. \quad (9)$$

At small-to-moderate offsets x , this expression approximates equation (4), whereas at large offsets, the 1 in the denominator of the final term becomes negligible so that the x^4 dependence becomes an x^2 dependence, with a coefficient such that the last two terms above yield the correct limiting velocity. The parameter A_5 is shown in the Appendix to be

$$A_5 = \frac{-A_4 V_{c2}^2}{\left(1 - \frac{V_{c2}^2}{V_{p2}^2}\right)}. \quad (10)$$

Hence, A_5 does not constitute a new free variable but is fully determined by the other variables already cited. So at no extra cost, equation (9) has the correct limiting behavior at both short and long offsets and varies smoothly in between. Tsvankin and Thomsen (1994) discuss a similar approximation for pure-mode P -wave propagation at some length, as do Dellinger et al. (1993).

CONVERSION POINT OFFSET: HOMOGENEOUS AND ISOTROPIC

Using elementary trigonometry in the simple case of Figure 1, it is easy to see that the source-receiver offset x_c of the C -wave conversion point is given by

$$x_c = V_p t_p \sin \theta_p = p V_p^2 t_p. \quad (11)$$

Hence, as a fraction of the total offset [equation (3)], the conversion point is (exactly)

$$\frac{x_c}{x} = \frac{1}{1 + V_s^2 t_s / (V_p^2 t_p)} = \frac{1}{1 + \frac{t_s(x)}{\gamma^2 t_p(x)}}. \quad (12)$$

Since both the oblique one-way times t_p and t_s are complicated functions of x , this relation is much more complicated than it looks. However, in the asymptotic limit of vertical travel (i.e., of small values of offset divided by thickness x/z), the ratio of traveltimes becomes

$$t_s(x)/t_p(x) \rightarrow t_{s0}/t_{p0} = V_p/V_s = \gamma$$

so that, in this limit, the asymptotic conversion point (ACP) is (Tessmer and Behle, 1988)

$$x_{c0} = \frac{x\gamma}{1 + \gamma}. \quad (13)$$

For larger offsets (or shallower depths), Tessmer and Behle (1988) express equation (12) explicitly as

$$\left[\frac{x_c(x - x_c)}{z}\right]^2 + \left[\left(x_c^2 - \frac{(2\gamma^2)}{(\gamma^2 - 1)}x(x_c - x/2)\right)\right] = 0. \quad (14)$$

In this arrangement, the limiting behaviors of the curve at both limits ($x/z \rightarrow \infty$ and $x/z \rightarrow 0$) are obvious from the separate solutions which follow directly from the neglect of one term or the other.

Tessmer and Behle (1988) also derive the exact solution of this equation; it is shown in Figure 2 for the special case of $\gamma = 2$. Here their exact solution is shown (solid) as well as some schematic raypaths, converting at various points (x_c, z). The vertical dotted line is, of course, the midpoint, where all of these rays would reflect if they did not convert but remained P -waves throughout.

The vertical dashed line is the ACP x_{c0} , [equation (13)]. It is clear from the figure that the actual conversion points at finite x/z differ significantly from this, especially at and shallower than $x/z = 1$, where most exploration interest lies. (In the past, we generally defined our maximum offsets to be close to the target depth, although longer offsets are becoming routine as we search for amplitude versus offset leverage.) The figure also contains an approximate curve and a Taylor curve, discussed below.

Looking at the same calculation from a different point of view, we can regard the solution of equation (14) as a function of x/z , this time with z fixed (i.e., we concentrate on a single event) and x varying from 0 to x_{\max} . In fact, it is common, for velocity determination purposes, to bin together traces with this range of offsets, all with a common value of the ACP x_{c0} . In

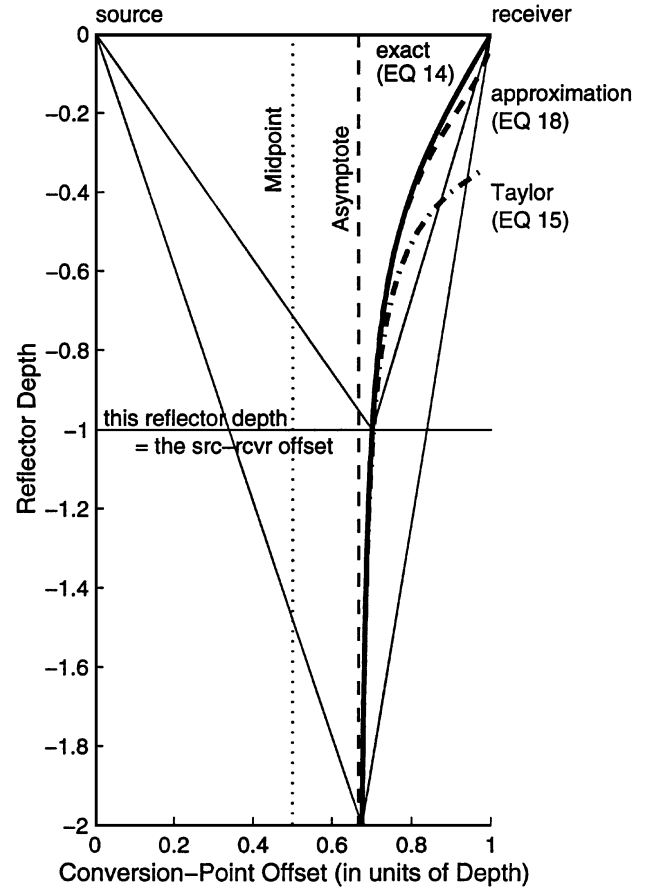


FIG. 2. Conversion-point offset as a function of reflector depth, with source-receiver offset fixed, i.e., for a single trace; $\gamma = 2.0$. The solution to equation (17) is noted by the dot-dashed curve.

such a common asymptotic conversion point (CACP) gather, the actual reflection points are smeared between this point x_{c0} and the actual values for $x_c(x)$. Figure 3 shows the resulting displacement of the actual conversion points from the asymptotic point, $x_c - x_{c0}$, and Figure 4 shows the corresponding raypaths.

How large is this offset from the asymptotic conversion point x_{c0} in actual meters? In a modern marine survey, the maximum offset x may be on the order of 4 km, with the target at a similar depth ($x_{max}/z = 1$). In recent clastic sediments, γ may be close to 3. Using these numbers in equation (14), we find that the

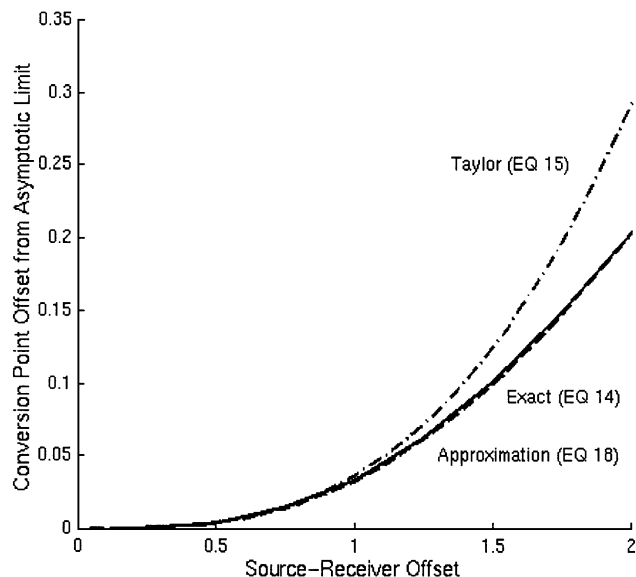


FIG. 3. Offset of the actual conversion point from its asymptotic limit as a function of source-receiver offset for a single event, i.e., within a CACP gather; $\gamma = 2.0$.

smear, $x_c - x_{c0}$, reaches 187 m for the receivers at the end of the spread. This means that if we were to regard that arrival as imaging the conversion point at x_{c0} instead of at x_c , we would misplace that energy by many bins. This is not a negligible smear, in most cases.

If the acquisition is split spread (as is easy to achieve on land or at sea with an OBS survey) with the same maximum offset in each direction, the smear is just twice that calculated above, distributed symmetrically about the CACP. Further, since in this context the normal-incidence reflectivity is zero (Aki and Richards, 1980), the traces at the distal ends of this smeared region have the greatest amplitudes.

Hence, an acceptable procedure for computing stacked traces must honor the depth-dependent conversion point $x_c(x/z)$, e.g., through the calculation of common conversion-point stacks (see below). To think about the differences from asymptotic behavior, it is useful to have an analytic solution to equation (14) that reveals some of the physics so we do not have to recompute opaque formulae for every case. In any case, we will need approximations for more realistic (multilayered, anisotropic) cases for which no exact solution is available.

In the Appendix, a Taylor expansion of the solution to equation (14) is derived, which is valid for small but finite values of x/z :

$$x_c(x, z) \approx x [C_0 + C_2(x/z)^2], \tag{15}$$

where the coefficients are given by

$$C_0 = \frac{\gamma}{1 + \gamma} \quad \dots \text{homogeneous, isotropic} \tag{16}$$

[see equation (14)] and

$$C_2(\gamma) = \frac{\gamma(\gamma - 1)}{2(\gamma + 1)^3} \quad \dots \text{homogeneous, isotropic.} \tag{17}$$

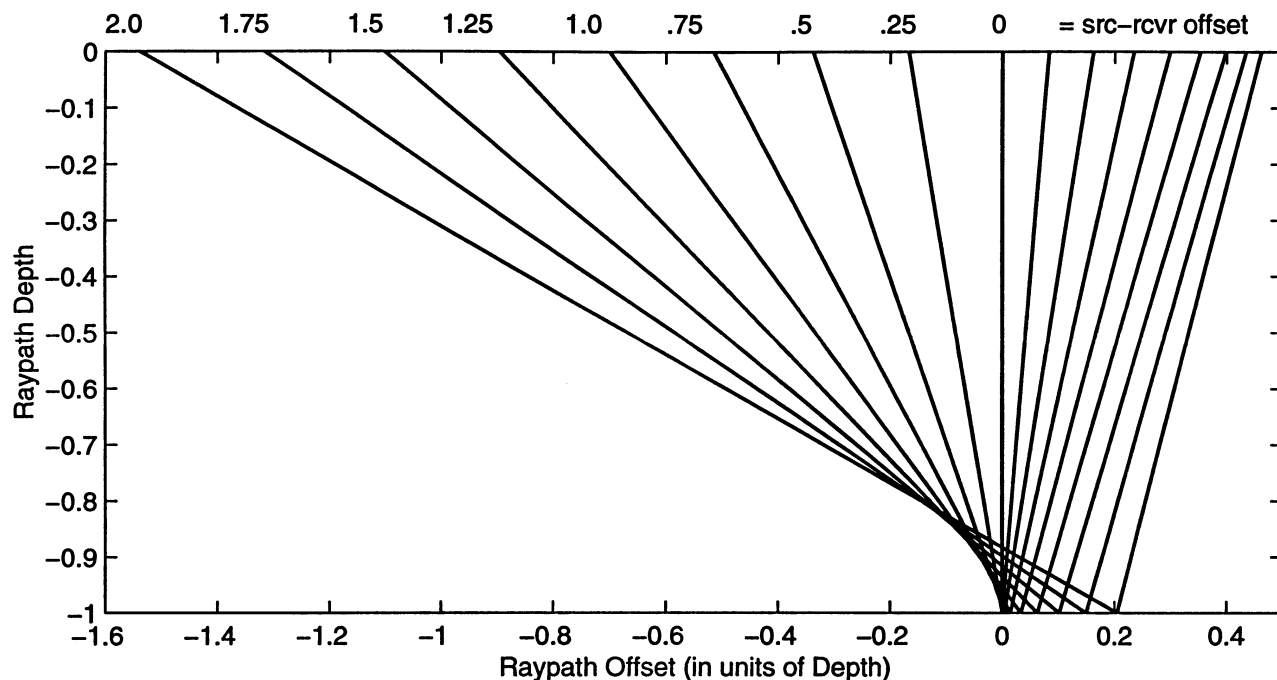


FIG. 4. Schematic raypaths for a single reflection event within a CACP gather.

This Taylor approximation solution is shown in Figure 2; it appears to be accurate for values of x/z as large as 1/0.8 but deviates strongly at larger offsets or shallower depths.

Hence, in the Appendix, a better approximate solution is also derived:

$$x_c(x, z) \approx x \left[C_0 + C_2 \frac{(x/z)^2}{(1 + C_3(x/z)^2)} \right], \quad (18)$$

with

$$C_3 = C_2/(1 - C_0). \quad (19)$$

Equation (19) has the same properties as equation (9): it is asymptotically correct at both limits ($x/z \rightarrow 0$ and $x/z \rightarrow \infty$) and varies smoothly in between. In Figure 2, this approximation is plotted as a dashed curve and is seen to be numerically accurate to values of x/z as large as 1/0.3. Rays reflecting from deep targets of exploration interest with these wide angles will not appear in most data sets, so these are acceptable errors. There is no strong advantage to this approximation (aside from the intuitive insight which it offers) in the simple case of Figure 1 (for which the exact solution of Tessmer and Behle, 1988, is available), but it will be quite useful in the more realistic cases discussed below.

MANY LAYERS

With the foregoing review and discussion of the essential features of the isotropic homogeneous case, we are now ready to consider more realistic cases. In a context of multiple layers, we must distinguish between the vertical velocity ratio function

$$\gamma_0 \equiv \bar{V}_p/\bar{V}_s = t_{s0}/t_{p0}, \quad (20)$$

where the bar indicates the average velocities, e.g., $\bar{V}_p(z) = z/t_{p0}(z)$, and the moveout velocity ratio function

$$\gamma_2 \equiv V_{p2}/V_{s2}, \quad (21)$$

where V_{p2} is the short-spread (rms) P -wave moveout velocity and V_{s2} is the S -wave equivalent.

The moveout equation in this case is equation (9), with both parameters V_{c2} and A_4 selected by flattening procedures, as described (in the P -wave context) by Tsvankin and Thomsen (1994). Equation (5) for the C -wave vertical traveltimes t_{c0} generalizes to

$$t_{c0} = t_{p0} + t_{s0} = t_{p0}(1 + \gamma_0). \quad (22)$$

The C -wave moveout velocity, equation (6), generalizes at every vertical time t_{c0} to

$$V_{c2}^2(t_{c0}) = \frac{V_{p2}^2}{1 + \gamma_0} + \frac{V_{s2}^2}{1 + 1/\gamma_0} = \frac{V_{p2}^2}{1 + \gamma_0} \left(1 + \frac{1}{\gamma_{eff}} \right), \quad (23)$$

where

$$\gamma_{eff} = \gamma_2^2/\gamma_0. \quad (24)$$

This is exactly equivalent to the much more complicated-appearing expression for migration velocity derived by Harrison and Stewart (1993). It does not reduce to equation (7), except in special cases of little practical interest.

These various velocity ratios may be found directly from P -wave and C -wave data once corresponding events have been identified. This correspondence, subject to some interpretation, is not usually a problem as regards the major reflectors, but it may be very difficult on a finer scale. Fortunately, the grosser scale correspondence is more crucial for velocity determination.

The vertical ratio γ_0 is found directly [cf. equation (22)] from the ratio of corresponding P - and C -vertical times (on stacks or extrapolated from oblique times on prestack gathers). Of course, to form a C -wave CACP gather, an initial guess for γ_{eff} is required [see equation (27) below]; hence, some iteration is normally required.

Then moveout velocity analysis is performed on both P -wave and C -wave data independently, determining V_{p2}^2 and V_{c2}^2 at corresponding times. Inverting equation (23)

$$\gamma_{eff} = [(1 + \gamma_0)(V_{c2}^2/V_{p2}^2) - 1]^{-1}. \quad (25)$$

The value γ_2 may then be found, if necessary, from equation (24). Given the different definitions of velocity ratio, clearly the moveout parameter for the C -wave should be chosen as the velocity V_{c2} itself, independent of P -wave data, rather than as some joint P/S parameter. The various velocity ratios should then be found subsequently to compute common conversion-point stacks, although some iteration is usually necessary.

A further advantage of this strategy is that since the determination of V_{c2} is virtually independent of any P -wave analysis, it is more robust than if some joint P/S quantity is estimated. In fact, to do this velocity analysis, one need not even have finally decided whether the conversion was at the reflector (C -mode), or perhaps at some other horizon, or have made a detailed correspondence between P -events and C -events.

For the many-layer case, the nonhyperbolic term in equation (9) is often nonnegligible at moderate offsets; the coefficient A_4 may be derived as an obvious special case of the anisotropic expression in Tsvankin and Thomsen (1994). However, the expression they give for A_4 need not be evaluated in practice; rather, A_4 may be determined empirically from the data, similar to the way V_{c2} is found, following the procedures recommended by Tsvankin and Thomsen (1994) for the corresponding P -wave case.

The C -wave conversion point offset, equation (18), generalizes (since the depths z are not known a priori in this more realistic case) as

$$x_c(x, t_{c0}) \approx x \left[c_0 + c_2 \frac{\left(\frac{x}{t_{c0} V_{c2}} \right)^2}{(1 + c_3(x/t_{c0} V_{c2})^2)} \right], \quad (26)$$

with

$$c_0 = \lim_{x \rightarrow 0} \frac{x_c}{x} = \frac{x_{c0}}{x} = \frac{\gamma_{eff}}{1 + \gamma_{eff}}, \quad (27)$$

[see equation (16)],

$$c_2 = \frac{\gamma_{eff} (\gamma_{eff} \gamma_0 - 1)(1 + \gamma_0)}{2\gamma_0 (1 + \gamma_{eff})^3}, \quad (28)$$

and

$$c_3 = c_2 / (1 - c_0) \quad (29)$$

(see the Appendix). The result for the ACP [equation (27)] appears in Chung and Corrigan (1985) without elaboration [see also Gaiser (1997)]; here it is seen as the asymptotic limit of a more general approximation. There, the velocity V_{s2} , which is embedded within γ_{eff} , is described as the shear rms velocity (referring in context to the vertical velocity structure); we shall shortly see that it is, in fact, more general than that.

Example from Valhall

As an example of the use of these equations, let us consider the Valhall OBS survey reported by Thomsen et al. (1997a). The ratio of vertical velocities inferred using equation (22) was $\gamma_0 = 2.9$, and the ratio of moveout velocities inferred from equations (24) and (25) was $\gamma_2 = 2.4$, yielding a value of $\gamma_{eff} = 2.0$. By naively ignoring possible effects of multiple layering and anisotropy (see below), the ACP would be calculated from the ratio of vertical traveltimes γ_0 to be at

$$\frac{x_{c0}}{x} = \frac{\gamma_0}{1 + \gamma_0} = 0.74.$$

By naively using the moveout velocity ratio γ_2 , it would be at

$$\frac{x_{c0}}{x} = \frac{\gamma_2}{1 + \gamma_2} = 0.70.$$

However, we properly calculate, using the effective ratio γ_{eff} for the conversion point [equations (25), (27)],

$$\frac{x_{c0}}{x} = \frac{\gamma_{eff}}{1 + \gamma_{eff}} = 0.66.$$

This is a significant difference from the naive approximations, amounting to several hundred meters at the furthest offsets. As we learn below, the differences between these various measures of velocity ratio, as seen in the Valhall data, may involve polar anisotropy as well as layering.

ACQUISITION

Especially in 3-D *C*-wave acquisition, consideration of the ACP is important to adequately define the full-fold, well-imaged area and to minimize the acquisition footprint. Of course, the ACP calculated from equation (27) using γ_{eff} should be used for this computation. To compute γ_{eff} , *C*-wave moveout must be observed [equation (25)], so an initial 2-D *C*-wave survey may be necessary to plan properly for a 3-D survey.

If log or vertical seismic profiling (VSP) information is used to determine γ_0 , and this is used in place of γ_{eff} to compute the ACP, significant shortcomings in resultant data quality may be expected because the full-fold area and the acquisition footprint depend upon the ACP through γ_{eff} , not γ_0 .

Further, it is not generally adequate to compute γ_{eff} by computing the *C*-wave moveout velocity from log or VSP data by calculating rms velocity values and then constructing V_{s2}^2 and V_{c2}^2 functions. The reason is that polar anisotropy also generally contributes to these moveout velocities; we will see that the formulae above are valid as written, even if the data contain the effects of polar anisotropy. These anisotropic effects are not, however, included in the vertical or near-vertical data

from logs and VSPs, so the computation of V_{c2}^2 from such input data can be expected to be imprecise.

Since the scalar reciprocity theorem is not valid for this vector data, 3-D acquisition and processing schemes that rely on this oversimplification may be in serious error. See below for a fuller discussion of the vector reciprocity theorem, which is, of course, valid.

TIME-DOMAIN STACKING

In a CACP gather, the actual conversion points $x_c(x, t_{c0})$ are smeared along a subsurface interval, as shown in Figure 4, according to source-receiver offset and the depth to the reflector. The higher amplitudes are normally concentrated near the end of this smear (or near both ends if the gather is split spread) because the normal-incidence conversion coefficient is zero and grows with increasing angle (Aki and Richards, 1980). This smear may be acceptable for determining the velocity parameters (depending on the lateral variation of velocity), but it is clearly unacceptable for imaging. In fact, Figure 4 shows that the shallower reflection events should actually image away from the CACP at significantly greater source-receiver offsets. Hence, a smeared, inaccurate image would result if a time-flattened CACP gather were to be simply added together at every time, as with *P*-waves.

Tessmer and Behle (1988) recommend a depth-variable rebinning procedure whereby at each particular flattened time t_{c0} the amplitude from each particular source-receiver offset x in the CACP is added to an address (in computer memory, corresponding to that same time and the true conversion-point offset). This address accumulates a stacked trace—positioned not at that CACP but at the true conversion point, calculated as the solution to equation (14). Of course, this procedure is subject to the assumptions of isotropy and vertical homogeneity implicit in that equation. Since the computation amounts to more than simple addition but actually moves energy about laterally, it is actually an approximate migration operation (see below).

A corresponding procedure, based on equation (26), is easy to implement and is far more general in its applicability. Given a flattened CACP gather, at each particular time t_{c0} , the amplitude from each particular source-receiver offset x is added to an address that accumulates a stacked trace—positioned not at the CACP but at the true conversion point, offset from the CACP (in the direction of the receiver) by the amount

$$\Delta x_c(x, t_{c0}) \approx \frac{x c_2 \left(\frac{x}{t_{c0} V_{c2}} \right)^2}{(1 + c_3 (x/t_{c0} V_{c2})^2)}. \quad (30)$$

In general, this computed conversion point lies between the discrete positions where stacks are to be calculated, so interpolation to those discrete points is necessary with different weights for each offset and each time, according to the distance to the two nearest discrete points. We see below that this procedure is valid even where the layers are anisotropic.

TIME-TO-DEPTH CONVERSION

The preceding formulae are given in terms of time rather than depth, since the arrival times are directly measurable whereas the depths must be inferred, usually with the help of an

assumption of isotropy. Time processing may be accomplished independent of such assumptions, so it is best to avoid them until they are needed. Eventually, of course, the conversion of time to depth must be made.

It seems obvious that depth determination should be done with P -waves instead of C -waves, but this may not be possible in practice, in some cases. To use C -waves to convert times to depths, we can follow the Dix procedure to transform stacking velocities to interval velocities in coarse layers and then add up the delays through each such layer, assuming the layers are isotropic.

We apply Dix differentiation to the C -wave hyperbolic moveout parameter [equation (9)], finding the (rms) average C -wave velocity between two coarsely spaced reflectors (labelled i and $i - 1$):

$$V_{ci}^2 \equiv \frac{t_{c0i} V_{c2}^2(t_{c0i}) - t_{c0i-1} V_{c2}^2(t_{c0i-1})}{t_{c0i} - t_{c0i-1}}. \quad (31)$$

As noted by Al-Chalabi (1974), this represents an rms average throughout the coarse interval rather than an arithmetic average. In the limit of very short waves, we would require the arithmetic average for t - z conversion; but since seismic waves do not typically meet this requirement anyway, we ignore these distinctions. It is shown in the Appendix that this leads to

$$V_{ci} = \frac{V_{pi}}{\sqrt{\gamma_{0i}}} \quad (32)$$

[compare with equation (7)]. Then, since the thickness of this isotropic layer is

$$\Delta z_i = V_{pi} \Delta t_{p0i} = V_{pi} \Delta t_{c0i} / (1 + \gamma_{0i}),$$

equation (32) yields

$$\Delta z_i = V_{ci} \Delta t_{c0i} \frac{\sqrt{\gamma_{0i}}}{1 + \gamma_{0i}}. \quad (33)$$

This provides the basis, through repeated application, for finding the total depth. In particular, one could use a C -wave velocity function in a conventional P -wave time-to-depth conversion routine to do this, after first stretching the C -wave velocity function by the time-variable factor given above. Of course, if the layers are anisotropic, new considerations arise.

LATERAL INHOMOGENEITY: DIODIC VELOCITIES

The preceding arguments have been limited, strictly speaking, to the case of lateral uniformity of velocity and structure, although (as with P -waves) modest and smooth lateral inhomogeneities are handled well. However, with C -waves in laterally inhomogeneous media, an additional feature arises because of the asymmetric raypath, and this deserves special mention here. In such media, C -wave arrival times and velocities are not invariant under an interchange of source and receiver positions, notwithstanding the apparent violation of the reciprocity theorem. We call this phenomenon diodic velocity, a term recalling the electronic diode, which operates differently in forward and reverse.

To make the argument simple and clear, consider Figure 5, wherein the layer is uniform except for a zone of anomalously slow P -velocity. The C -wave traveling from \mathbf{A} to \mathbf{B} in the figure arrives sooner than the C -wave traveling from \mathbf{B} to \mathbf{A} , since only the latter traverses the slow zone as a P -wave. The arrival

time and effective velocity of the C -wave is not invariant under an exchange of source and receiver position if the source retains its vector character, and likewise for the receiver. The argument obviously remains valid for any general lateral inhomogeneity in velocity, including dipping reflectors.

This means a split-spread gather of traces showing C -wave arrivals through laterally heterogeneous media will not have symmetric moveout. If the sources are shot on the groups, then the sources (receivers) with positive offsets have the same positions as the receivers (sources) with negative offsets. One side of a split-spread common midpoint (CMP) gather has its source and receiver positions exactly exchanged (with respect to the other). Since the C -wave arrivals are diodic, the moveout will not be the same for the two sides, in general. Of course, this does not happen for P -waves or for any other pure-mode event.

The asymmetry appears also for split spreads shot between the groups, although some interpolation is required to confront the reciprocity theorem. The asymmetry also appears for a common conversion-point gather, although there is not an apparent violation of the reciprocity theorem.

Of course, the reciprocity theorem is not violated; it is valid for all elastic media, homogeneous or not, isotropic or not, with any mode(s) of propagation (see Knopoff and Gangi, 1959; Claerbout and Dellinger, 1987). However, it must be applied properly in vector fashion. It says that, given a source (body force per unit mass) $\mathbf{f}(\mathbf{A})$ applied at \mathbf{A} with a resultant displacement at \mathbf{B} given by $\mathbf{u}(\mathbf{A}; \mathbf{B})$ and a vector force $\mathbf{f}(\mathbf{B})$ applied at \mathbf{B} with resultant displacement at \mathbf{A} given by $\mathbf{u}(\mathbf{B}; \mathbf{A})$, the scalar products obey

$$\mathbf{f}(\mathbf{A}) \cdot \mathbf{u}(\mathbf{A}; \mathbf{B}) = \mathbf{f}(\mathbf{B}) \cdot \mathbf{u}(\mathbf{B}; \mathbf{A}). \quad (34)$$

In other words, the vector *projection* of the recorded signal upon the source direction at one point is identical to the same *projection* at the other point.

We may decompose (at each location) the recorded data vector into two components, which we label as *source-parallel* and *source-perpendicular*. The vector reciprocity theorem requires that the *source-parallel* components of data be identical; it does not constrain the *source-perpendicular* components in any way. For the situation in Figure 5, the data lie chiefly in this *source-perpendicular* direction and are largely unconstrained. The same is true in most OBS C -wave situations, where the velocity gradient in the near surface bends the rays nearly vertically and the recorded data components are nearly horizontal.

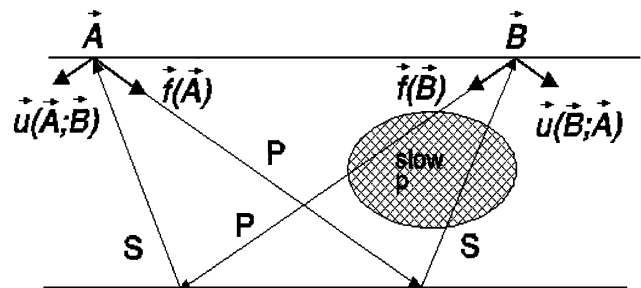


FIG. 5. Diodic velocity occurs for C -waves whenever there is lateral variation in velocity.

If, instead, the source $\mathbf{f}(\mathbf{B})$ were excited exactly parallel to $\mathbf{u}(\mathbf{B}; \mathbf{A})$ (i.e., nearly horizontally), then the recorded data $\mathbf{u}(\mathbf{A}; \mathbf{B})$ would lie nearly parallel to $\mathbf{f}(\mathbf{A})$ and the component exactly parallel to $\mathbf{f}(\mathbf{A})$ would exactly equal $\mathbf{u}(\mathbf{B}; \mathbf{A})$. This arrangement of the source $\mathbf{f}(\mathbf{B})$ amounts to sending the wave back the way it arrived along the reverse path (S - P), which of course is not a C -wave (by definition) and is hard to accomplish in practice.

A close approximation to the situation of Figure 5 is seen in the Valhall OBS survey (Thomsen et al., 1997a). Figure 6 shows a velocity spectrum and a split-spread CMP supergather from that survey, zoomed on the reservoir level and corresponding to a CMP location to one side of the Valhall gas cloud (slow P -zone). The near-offset traces are in the center of the gather; wide negative and positive far offsets are on either side. The velocity spectrum is clearly bimodal, with well-separated semblance maxima at times corresponding to the reservoir peaks. The velocity pick shown (the fast pick) has flattened the negative offsets, but the positive offsets are undercorrected. Alternatively, a pick of the slow velocity flattens the positive offsets and overcorrects the negatives. Far away from the gas cloud, the effect diminishes, then disappears. A similar effect, but with reverse polarity, occurs on the other side of the gas cloud. In this instance, the fact that the OBS receiver is 64 m deeper than the air gun source is irrelevant to the discussion. A CACP gather shows the same asymmetry.

In cases where the velocity heterogeneity is less pronounced, the bimodal semblance maxima smear together and appear as one poorly resolved peak. Even then, the velocity resolution and consequent image quality may be substantially increased by explicitly recognizing the diodic nature inherent to C -wave velocity.

One consequence of the phenomena of diodic velocity is that, in laterally inhomogeneous media, neither the nonhyperbolic moveout equation (9) nor its hyperbolic restriction (with $A_4 = 0$) is strictly valid. The reason is that interchanging source and receiver positions amounts to reversing the sign of the offset x in the equation. But since the equation is even in x , the sign of x is immaterial to the result, so this theory cannot account for data showing diodic velocity (it was, after all, derived for the case of lateral homogeneity).

In 2-D surveys, there are trivial ways to sidestep this problem. For example, a simple procedure is to process each one-sided gather independently and to join the images at a place of convenience (Thomsen et al., 1997a). In such a case, the correct positioning of the conversion points (using the procedure outlined above) is crucial to obtain a proper join.

However, in 3-D surveys the problem is far from trivial, is not addressed in the literature, and requires a true vector solution. If a CACP-binned gather from a 3-D survey is sorted by source-receiver unsigned offset (radius), this would correspond to folding together the two sides of Figure 6. An inexperienced processor might completely misinterpret the bimodal velocity spectrum, not realizing the physical reason for the two peaks. If the semblance peaks are overlapping, then this is especially likely. In both cases, inaccurate imaging would probably result.

CONVERTED-WAVE AVO

Analysis of converted-wave amplitudes and their variation with offset (C -AVO) involves all of the considerations, familiar in P -wave AVO studies, required to convert received amplitudes into true relative amplitudes that provide reflectivity as a function of incident angle. These true relative amplitudes must then be converted into half-space reflection coefficients

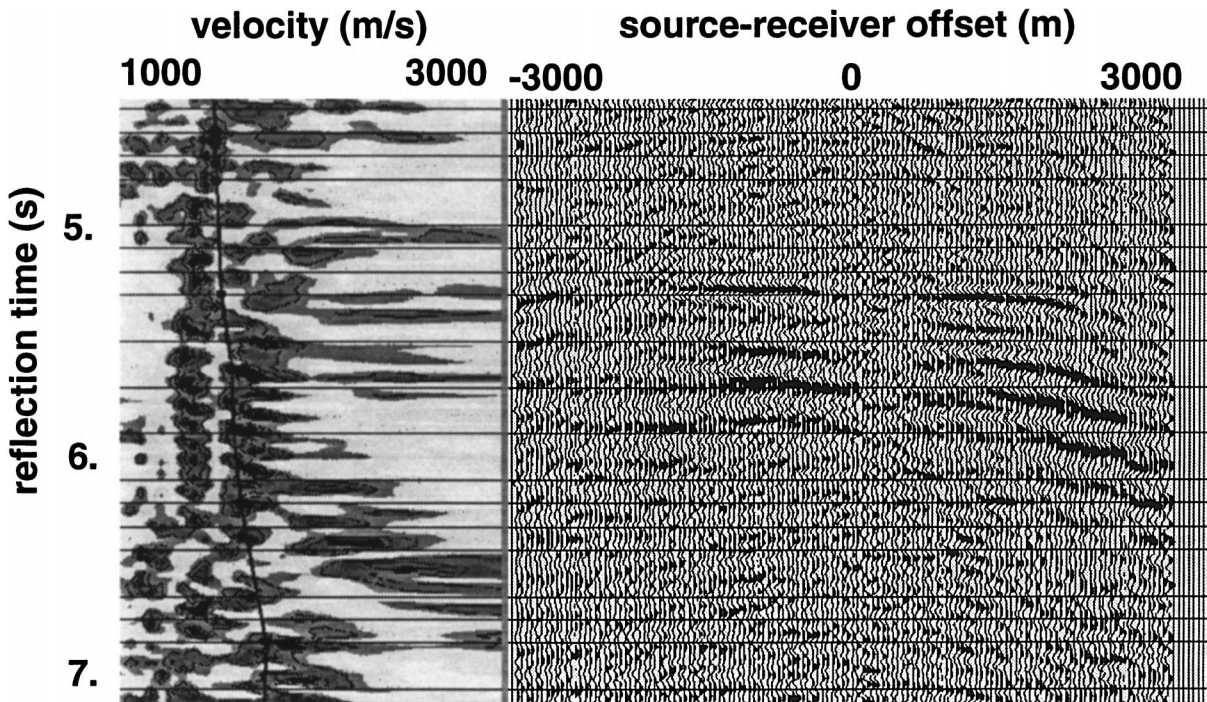


FIG. 6. An asymmetric split-spread CMP supergather (inline horizontal component) from Valhall at the target level, showing diodic velocity character. A velocity spectrum is shown on the left; the supergather is on the right.

(free of thin-bed interference effects), which can then be the subject of physical interpretation. All of these considerations lie outside the scope of the present work but are generally analogous to the corresponding considerations in P-AVO.

However, a new consideration peculiar to C-AVO studies must be addressed even before a set of traces is ready for the procedures mentioned above. One must first construct a true common conversion-point (CCP) gather, unstacked (as opposed to a CACP gather), so all amplitudes of a given event refer to conversion at a single point in space without the smear shown in Figure 4. The time domain stacking procedure mentioned above of course destroys all C-AVO effects in accumulating the stacked CCP trace.

However, a simple modification to those procedures preserves the necessary information. Consider that the flattened CACP gathers at all CACP positions x_{c0} , with offsets x and flattened times t_{c0} , have amplitudes $s(x_{c0}, x, t_{c0})$. We wish to construct flattened CCP gathers, each with a common conversion point x_c for all events (all times t_{c0}) and all offsets, $s(x_{c0}, x, t_{c0})$. We can do that by mapping the array $s(x_{c0}, x, t_{c0})$ into a new array $s(x_c, x, t_{c0})$; the mapping function is given by equation (26) or, equivalently, equation (30). It is exactly the time domain stacking procedure, except that the CCP amplitudes are not added together; instead, the C-AVO behavior is preserved for analysis.

The exact reflection coefficient for C -waves at a planar boundary is discussed by Aki and Richards (1980) for the isotropic case. In their linearized form (small elastic contrasts), these equations assume a form analogous to the linearized P -wave reflectivity with three notable features.

- 1) The angular dependence is odd (rather than even) in incident angle θ so that interchanging source and receiver positions in the flat-lying geometry of Figure 1 reverses the algebraic sign of the received amplitude. This is related to the discussion of diodic velocities. In 2-D split-spread surveys, the trivial remedy is to reverse the polarity of one-half of each split-spread gather and proceed. However, in wide-azimuth surveys a true vector solution is required.
- 2) Because of the foregoing, the essential parameters in C-AVO analysis are the slope and curvature of the C-AVO function, rather than the intercept and slope, as in P-AVO analysis.
- 3) The coefficients in the linearized expressions depend upon the jumps in density and shear velocity only and not upon the jump in P -velocity. This means that the well-known nonlinear dependence of P -wave reflectivity upon gas (or other light hydrocarbon) in the pore space near the reflector does not enter into the quantitative analysis of C-AVO. This in turn means that such data, perhaps jointly with P-AVO, may in principle be quantitatively analyzed for gas saturation, thereby offering a solution to the "fizz-gas" problem.

ANISOTROPIC CONSIDERATIONS: POLAR ANISOTROPY

Since all of these results depend upon γ , and since γ depends strongly on direction in an anisotropic medium, it is clear that we need to consider this case explicitly. From Tsvankin and Thomsen (1994), we deduce that, since c_0 and c_2 depend only on the short-spread moveout parameters t_{c0} and V_{c2} , we can

use equations (20–30) as written, so long as we recognize that the measured moveout velocities V_{p2} and V_{s2} are those affected by both the layering and the anisotropy [equations (A-3) and (A-4)]. This is trivial since the data have these effects in them already.

Note: Francis Muir independently derived the result, equation (27), for c_0 for a homogeneous anisotropic layer several years ago (personal communication) and presented it to the Stanford Exploration Project sponsors but never formally published it.

The seismic parameters defined above lead to the correct displacement of the conversion point, even if the differences between γ_0 and γ_2 arise from anisotropy as well as many layers. The separate contributions attributed to layering and anisotropy may be estimated using the detailed formulae for V_{c2} given by Tsvankin and Thomsen (1994), although this is not necessary for time processing.

As a simple special case, if the difference between γ_0 and γ_2 is ascribed completely to anisotropic effects (neglecting layering effects), we can directly estimate the anisotropy parameters δ and σ (see the Appendix). The anisotropic parameter δ is given by the difference between vertical and moveout P -wave velocities (Tsvankin and Thomsen, 1994). Hence, if we know the vertical P -wave traveltime and the depth (i.e., from borehole information), we calculate V_{p0} and, hence, δ . Then the anisotropic parameter σ is given from

$$\gamma_{eff} = \frac{\gamma_2^2}{\gamma_0} = \gamma_0 \frac{(1 + 2\delta)}{(1 + 2\sigma)}.$$

Since σ is often greater than δ , it follows that γ_{eff} is often less than γ_0 in cases where the difference is caused by anisotropy. This has the effect of moving the image point closer to the source than for an isotropic medium with the velocity ratio γ_0 . This is consistent with the modeling work of Eaton (1993).

If the C -wave hyperbolic moveout coefficients V_{c2} are affected by polar anisotropy, then the interval C -wave velocity, produced by the Dix differentiation [equation (31)], is (see the Appendix)

$$V_{ci}^2 = V_{pi}^2 \left(\frac{1 + 1/\gamma_{ci}}{1 + \gamma_{0i}} \right), \quad (35)$$

where

$$\gamma_{ci} = \gamma_{0i} \frac{(1 + 2\delta_i)}{(1 + 2\sigma_i)}. \quad (36)$$

This reduces, of course, to equation (32) if the layer anisotropies δ_i and σ_i are zero. Then the layer thickness [equation (32)] becomes

$$\Delta z_i = V_{ci} \Delta t_{0i} [(1 + \gamma_{0i})(1 + 1/\gamma_{ci})(1 + 2\delta_i)]^{-1/2}. \quad (37)$$

The use of this equation to calculate thicknesses and, by repetition, depths is obviously more problematic than in the isotropic case [equation (33)]. In principle, one could apply the stretch factor given above to velocities of a C -wave velocity function, but this does not answer the question of determining the values of the anisotropy parameters.

USE OF ISOTROPIC COMPUTER CODES

The previous results raise the question of whether it is possible to use code written with the assumption of isotropy to process data from an anisotropic medium. Of course, we do

this all of the time with P -wave data; the anisotropy is hidden within the moveout velocity and manifests itself first as time-to-depth mis-ties. If we avoid long spreads with nonhyperbolic moveout and confine our AVO analysis to qualitative techniques, this approach works quite nicely.

In the C -wave context, we also have the consideration of the conversion point. It is clear from equation (27) that the asymptotic conversion point x_{c0} will be calculated properly by such an isotropic program if we tell it that the velocity ratio function is given numerically by γ_{eff} . (This assumes the program does not find its own velocity ratio internally.)

However, it is also clear from equation (28) that the departure of the actual conversion point from the ACP involves other quantities. Let us write the coefficient c_2 , which controls this departure, for an isotropic medium with velocity ratio $\gamma = \gamma_{eff} = \gamma_0$:

$$c_2^{iso}(\gamma_{eff}) = \frac{(\gamma_{eff} - 1)}{2(\gamma_{eff} + 1)}. \quad (38)$$

Then the actual coefficient [equation (28)] suitable for the many-layered, anisotropic context may be rewritten as

$$c_2 = c_2^{iso}(\gamma_{eff}) \left[\frac{\gamma_{eff} (\gamma_{eff} \gamma_0 - 1)(\gamma_0 + 1)}{\gamma_0 (\gamma_{eff}^2 - 1)(\gamma_{eff} + 1)} \right]. \quad (39)$$

With this equation, one may make an informed judgment about the degree of approximation involved in setting the factor in brackets to unity in any particular case. In most cases, this will likely prove to be an acceptable approximation. Where it is acceptable, this makes a substantial simplification to processing, for then one can use an isotropic code simply by supplying it with the proper value of the $\gamma_{eff}(z)$ function. Where this approximation is unacceptable, isotropic codes will lead to errors.

Alternatively, an isotropic program may calculate the conversion point using an adaptation of Tessmer and Behle's (1988) equation in terms of x/z , using P -wave times to determine the depths. To analyze this situation, we use equation (18), which shows the depth explicitly, with C_0 given by equation (28), C_3 given by equation (19), and

$$C_2 = \frac{\gamma_{eff}^2 (\gamma_{eff} \gamma_0 - 1) (\overline{V_p})^2}{2\gamma_0 (1 + \gamma_{eff})^4 V_{p2}^2}. \quad (40)$$

The isotropic coefficient in this case is [equation (17)]

$$C_2^{iso}(\gamma_{eff}) = \frac{\gamma_{eff} (\gamma_{eff} - 1)}{2 (\gamma_{eff} + 1)^3}, \quad (41)$$

in terms of which the actual coefficient may be written

$$C_2 = C_2^{iso}(\gamma_{eff}) \left[\left(\frac{\gamma_{eff} (\gamma_{eff} \gamma_0 - 1)}{\gamma_0 (\gamma_{eff}^2 - 1)} \right) \frac{(\overline{V_p})^2}{V_{p2}^2} \right]. \quad (42)$$

For this situation, equation (42) may be used to estimate whether such an isotropic program offers sufficient accuracy in any particular case. If the quantity in brackets is close to one, then the subsurface may be analyzed in this quasi-isotropic way, utilizing $\gamma_{eff}(z)$ in an isotropic code. Where this approximation is not acceptable, isotropic codes will lead to errors.

MIGRATION, DMO

Of course, the stacking procedures discussed herein are loaded with approximations and may be supposed to be inherently inferior to migration procedures. However, migration has its own approximations, and these may prove to be even more troublesome. In particular, it is quite clear from the foregoing simple analysis that whenever polar anisotropy is present, a valid migration should include those effects. It is common for shear-wave anisotropy to be greater than P -wave anisotropy (i.e., σ is greater than δ), so the net effect on C -waves may be expected to be greater than we commonly experience in P -wave exploration. In particular, the requirement for true depth determination (for joint P/C -wave interpretation) is made much more difficult when anisotropy prevents true depth determination for either the P -waves or the C -waves.

In such cases, approximate time-based processing may be more appropriate. The simple formulae derived herein yield important insights that are often precluded by more exact formulations. However, the time-migration operator for layered, polar-anisotropic media may be derived following principles similar to those used here [equation (9)]. In fact, the function $x_c(t_{c0}, x)$ from equation (26) may be viewed as an approximation to the zero-aperture (zero-dip) time-migration operator.

For purposes of partial migration or dip moveout (DMO), a solution (for the isotropic homogeneous case of Figure 1) is given by Alfaraj (1993), using a modification of Hales' (1984) f - k method. It utilizes a reflection time-variant phase shift applied to NMO-corrected data to track the movement of the conversion point x_c , as shown (for the flat-lying case) in Figure 2. This method may also be generalized to deal with anisotropic, layered media following the principles described herein.

ANISOTROPIC CONSIDERATIONS: AZIMUTHAL ANISOTROPY

Most rocks are azimuthally anisotropic to some degree. This means the converted shear waves are not polarized in the vertical plane (so-called SV -waves) as commonly assumed. Instead, they are split into two S -waves, polarized in two directions. These two directions are determined by the material and the ray direction, rather than by the source (the source polarization only determines the relative excitation of the two natural polarizations). The two polarizations travel at slightly different velocities, so they split in their arrival times. In general, both are registered on both in-line and cross-line receivers.

Since the two shear velocities are usually very close to each other (usually within $\sim 2\%$), we can still use most of the foregoing analysis of moveout and conversion points. However, we usually need further analysis to cope with the split arrivals, since each reflector generally gives rise to at least two arrivals, and these will confuse the interpretation unless corrected for. [A second source of confusion may arise if two shear arrivals are generated because of wave-surface concavity in polar-anisotropic media (Ohlsen and MacBeth, 1996). Because of the steeply dipping shear leg in a C -mode (Figure 1), this phenomenon is not likely to present itself in this context.]

The primary analysis of such shear-wave splitting is given in Thomsen (1988) and references cited therein and so is not repeated here. In applying that material to the present case, one need only recall that an obliquely traveling P -wave excites

the reflected shear wave with an in-line excitation, which is discussed explicitly there. The reflection angle θ_r [equation (1)] is smaller than in the corresponding shear case because of the displacement of the conversion point from the midpoint. Further, the obliquely traveling shear wave coming up bends more vertically (than shown in the figure) as it reaches the surface (from Snell's law and the general decrease of velocities with decreasing depth). Hence, the vertical propagation analysis given in Thomsen (1988) is probably an adequate approximation—even more adequate than for propagation.

On the other hand, particularly if the *C*-wave data is from an OBS survey, there may be valid questions concerning the equality of sensitivity of the various vector components, i.e., concerning *vector fidelity*. We wish to treat the various components as parts of a vector—for example, by rotating them vectorwise. This obviously requires that the instrument response in both amplitude and phase, including coupling effects, is the same for all components. Land geophones have had sufficient developmental history so we are relatively comfortable with concluding that these component responses are equivalent. The same is not currently true of OBS receivers. So in considering the algorithms discussed below, we should remember that they assume the data is a true vector and the various components may be manipulated as such—an assumption that should be viewed in practice with scepticism (Thomsen et al., 1997b).

In land shear-wave exploration, it is common to use both in-line and cross-line sources, recording into both in-line and cross-line receivers, yielding a 2×2 tensor of data (Thomsen, 1988). In the 2-D *C*-wave problem, we have only a two-vector of data, so we cannot perform tensor (Alford) rotation but must use vector rotation, as described conceptually in Thomsen (1988).

Harrison (1992) implements these ideas by incorporating several additional assumptions not present in Thomsen (1988):

- 1) The slow-shear wavelet is identical to the fast-shear wavelet in amplitude (Harrison, 1992). This assumption is not fulfilled in the general case since the effective shear-modulus contrast (across the reflecting horizon) is different for each polarization.
- 2) The slow-shear wavelet is identical to the fast-shear wavelet in phase (Harrison, 1992). This assumption is not fulfilled in the general case since the attenuation for the fast mode may be different than for the slow mode, although we often find them comparable in field data.
- 3) The pure-mode autocorrelation can be estimated from the total autocorrelation function of the data (Harrison, 1992, p. 32).

For 3-D *C*-wave surveys, new possibilities arise. If we consider, as a transition to three dimensions, the case of orthogonally crossing 2-D *C*-wave lines, we see that at the tie point, i.e., at the common conversion point on each line corresponding to the intersection point, we have Alford's problem: two orthogonal polarizations of sources with two orthogonal receivers recording each. Hence, we can apply tensor rotation to this four-part data set; it should prove much more robust than the vector rotation described above.

In wide-azimuth 3-D surveys, it is common to have in every common conversion-point bin a collection of traces with a wide variety of offsets and azimuths. It is common to project the horizontal components from each shot onto its source-receiver

azimuth and to handle the resulting calculated radial data as scalar data by forming CACP-binned gathers of such traces. However, this procedure is suggested by the assumption of azimuthal isotropy; normally it is only necessary to observe the significant coherent energy present on the calculated transverse components to realize that this assumption is invalid and that a more realistic approach is required.

From this collection of traces with many offsets and azimuths, one can use a least-squares (or other statistical) procedure to deduce the azimuth of orientation of the principal coordinate system onto which this redundant data can best be projected, yielding an Alford-type interpretation of the anisotropy. One approach to doing this, subject to assumptions about the distribution of source-receiver azimuths and offsets, is given by Garotta and Granger (1988); another is given by Gaiser (1997). Such a procedure, or one more elaborate, appears to be necessary in most cases.

Most of the discussion of shear-wave splitting in the literature assumes uniform (with depth) orientation of the principal directions of azimuthal anisotropy. In cases where the orientation varies with depth, the formalism established by Thomsen et al. (1999) may be useful.

CONCLUSIONS

An essential part of the analysis of any converted-wave data set is determining where the conversion occurs; this paper deals only with conversion ($P \rightarrow S$) at the reflector.

Because the image point offset of such *C*-waves must be calculated on physical grounds rather than on geometrical grounds (even in the simplest geometry), the role of physical properties in *C*-wave processing is much more pronounced than in *P*-wave processing. Hence, simple physical characterization such as isotropy or spatial homogeneity can impede *C*-wave imaging, whereas for *P*-waves it can often be postponed to follow the imaging. In fact, *C*-wave acquisition, processing, and interpretation should proceed together for greatest effectiveness.

Simple, data-driven approximate formulae enable (1) the calculation of the *C*-wave image point in the minimally realistic case of vertical inhomogeneity (layering), and polar anisotropy, and (2) the computation of time-domain stacks and unstacked common conversion-point gathers using the true (time-dependent) conversion point. The computation of the conversion-point offset is best done in terms of time rather than depth since the depths are imprecise in the presence of anisotropy. At Valhall (Thomsen et al., 1997a), the differences between this computation and a naive computation using the assumption of isotropic homogeneity and the vertical velocity ratio are significant for imaging precisely enough for efficient exploitation of the reservoir. The use of these formulae is important even in the acquisition planning stage to properly illuminate the area to be imaged and to avoid serious acquisition footprints.

C-wave velocities are inherently *diodic*, that is, they depend upon the direction of the source \rightarrow receiver vector and are *not* invariant under exchange of source and receiver positions if the media are laterally inhomogeneous and/or azimuthally anisotropic—i.e., if the survey is performed in the real world. This does not violate the vector reciprocity theorem. It does complicate velocity analysis, particularly in 3-D surveys, where

a sort of gathered traces from a CACP bin, if ordered by unsigned radius only, ignores this fundamental feature.

The use of computer codes based on isotropic algorithms can often be successful if they are deceived in appropriate ways, given herein. The errors consequent to such deception may be estimated by evaluating the anisotropic correction factors given above. The anisotropic correction factors may be derived from the data itself.

Since most sedimentary rocks are azimuthally anisotropic, the upcoming *S*-leg of the *C*-wave will usually be split into (at least) two events per reflector, polarized in the principal directions preferred by the medium (not determined by the source). It is usually important to separate the data, as recorded, into different components that each contain one event per reflector (either fast or slow). This requires determining of the principal directions. In 2-D surveys, the two horizontal components constitute a sufficient, albeit marginal, 2×1 data set for determination of these principal directions. In wide-azimuth 3-D surveys, one can construct a more robust algorithm via a statistical approximation to Alford's orthogonal-source-excitation 2×2 matrix.

ACKNOWLEDGMENTS

I thank Amoco Exploration and Production for permission to publish this material and Amoco's Multicomponent Seismic Team (O. Barkved, G. Beaudoin, B. Haggard, J. Kommedal, M. Mueller, and B. Rosland) for many stimulating discussions about the data which drove these concepts.

REFERENCES

- Aki, K., and Richards, P., 1980, Quantitative seismology: Freeman Press.
 Al-Chalabi, M., 1974, An analysis of stacking, RMS, and interval velocities over a horizontally layered ground: *Geophys. Prosp.*, **22**, no. 3, 458.

- Alfaraj, M., 1993, Transformation to zero offset for mode-converted waves: Ph.D. thesis, Col. School of Mines.
 Alkhalifah, T., and Tsvankin, I., 1995, Velocity analysis for transversely isotropic media: *Geophysics*, **60**, 1550–1566.
 Claerbout, J., and Dellinger, J., 1987, Eisner's reciprocity paradox and its resolution: *The Leading Edge*, **6**, 34–37.
 Chung, W. Y., and Corrigan, D., 1985, Gathering mode-converted shear waves: A model study: 55th Ann. Internat. Mtg., Soc. Expl. Geophys., Expanded Abstracts, 602–604.
 Dellinger, J. A., Muir, F., and Karrenbach, M., 1993, Anelliptic approximations for TI media: *J. Seis. Explor.*, **2**, 23–40.
 Eaton, D., 1993, Processing of converted-wave data from VTI media: Ph. D. thesis, Univ. of Calgary.
 Gaiser, J. E., 1997, 3-D converted shear wave rotation with layer stripping: U.S. Patent, 5 610 875.
 Garotta, R., and Granger, P. Y., 1988, Acquisition and processing of 3-C \times 3-D data using converted waves: 58th Ann. Internat. Mtg., Soc. Expl. Geophys., Expanded Abstracts, S13.2.
 Hale, D., 1984, Dip-moveout by Fourier transform: *Geophysics*, **49**, 741–757.
 Harrison, M., 1992, Processing of P-SV Surface-Seismic Data: Anisotropy Analysis, Dip Moveout, and Migration, Ph.D. Thesis, Univ. of Calgary.
 Harrison, M., and Stewart, R., 1993, Poststack migration of *P-SV* seismic data: *Geophysics*, **58**, 1127–1135.
 Knopoff, L., and Gangi, A. F., 1959, Seismic reciprocity: *Geophysics*, **24**, 681–691.
 Ohlsen, F., and MacBeth, C., 1996, Unexpected shear-wave double-reflection: 66th Ann. Internat. Mtg., Soc. Expl. Geophys., Expanded Abstracts, **58**, 1951–1954.
 Tessmer, G., and Behle, A., 1988, Common reflection point data-stacking technique for converted waves: *Geophys. Prosp.*, **36**, 671–688.
 Thomsen, L., 1988, Reflection seismology over azimuthally anisotropic media: *Geophysics*, **51**, 304–313.
 Tsvankin, I., and Thomsen, L., 1994, Nonhyperbolic reflection moveout in anisotropic media: *Geophysics*, **59**, 1290–1304.
 Thomsen, L., Barkved, O., Haggard, B., Kommedal, J., and Rosland, B., 1997a, Converted-wave imaging of Valhall reservoir: 59th Mtg., Europ. Assoc. Geosci. Engrs., Expanded Abstracts, B048.
 ——— 1997b, A study of the dependence of OBS data-quality on seafloor equipment: Draggged-versus and cable data: Presented 67th Ann. Internat. Mtg., Soc. Expl. Geophys., Research Workshop on 4C Applied Technology (cf. <http://4c.seg.org/thomsen.html>).
 Thomsen, L., Tsvankin, I., and Mueller, M. C., 1999, Coarse-layer stripping of shear-wave data for vertically variable azimuthal anisotropy: *Geophysics*, **64**, in press.

APPENDIX

DERIVATIONS

Moveout: anisotropic layers

We first consider the various coefficients in the Taylor series [equation (4)]. The moveout velocity V_{c2}^2 is given by the methods of Tsvankin and Thomsen (1994) as equation (23). Note that the distinction between ray angle and wavefront angle may be neglected in this context of near-offset derivatives.

If the layers are anisotropic, the short-spread moveout velocities are affected by the anisotropy. In each layer

$$V_{p2}^2 = V_{p0}^2(1 + 2\delta) \quad (\text{A-1})$$

and

$$V_{s2}^2 = V_{s0}^2(1 + 2\sigma), \quad (\text{A-2})$$

where V_{p0} and V_{s0} are the vertical velocities and δ and σ are two independent anisotropic parameters discussed by Tsvankin and Thomsen (1994). If there are many anisotropic layers, then the velocities V_{p0}^2 and V_{s0}^2 should be understood as rms vertical velocities and the anisotropy parameters δ and σ are also rms

averages, as discussed more fully by Tsvankin and Thomsen (1994).

The quartic parameter A_4 of equation (4) is given by Tsvankin and Thomsen (1994) in the single-layer case as

$$A_4 = \frac{-1}{(1 + \gamma_{eff})^2} \left[2\eta \frac{(\gamma_0^2 - 1)}{\gamma_0} \gamma_{eff}^2 + \frac{(\gamma_2^2 - 1)^2}{4(\gamma_0 + 1)} \right] \bigg/ V_{c2}^2 t_{c0}^2, \quad (\text{A-3})$$

where η is another anisotropic parameter defined by Alkhalifah and Tsvankin (1995) in terms of elementary anisotropy parameters by

$$\eta = \frac{(\varepsilon - \delta)}{(1 + 2\delta)}. \quad (\text{A-4})$$

As discussed by Tsvankin and Thomsen (1994) and Alkhalifah and Tsvankin (1995), η is determined in principle by nonhyperbolic *P*-wave moveout or by high-angle reflections from dipping reflectors, such as normal faults. For the multilayered anisotropic case, Tsvankin and Thomsen (1994) give A_4 as a combination of layer properties too gruesome to repeat here.

As discussed in the main text, the Taylor expansion [equation (4)] has the wrong asymptotic behavior; the refinement suggested by Tsvankin and Thomsen (1994) in the pure-mode context is more useful. Here we derive the refinement parameter A_5 , which appears in equations (9) and (10). As is apparent from Figure 2, at large relative offsets x/z the conversion-point offset x_c approaches the emergence offset x , so that the P -wave travels down nearly horizontally and the S -wave travels up nearly vertically. Thus, at large offsets, the time-offset relation should approach

$$(t(x) - t_{s0})^2 = t^2(1 - t_{s0}/t)^2 = \text{constant} + x^2/V_{ph}^2, \quad (\text{A-5})$$

where V_{ph} is the horizontal P -velocity. If we linearize t^2 in the small quantity t_{s0}/t , we find that even the linear term becomes negligible in comparison to the x^2 term at large offsets. Setting this expression equal to equation (9) at large offsets results in

$$t^2(x) \rightarrow t_0^2 + x^2/V_{c2}^2 + \frac{A_4 x^2}{A_5} \approx \text{constant} + x^2/V_{ph}^2 \quad (\text{A-6})$$

so that

$$A_5 = \frac{A_4}{\left(\frac{1}{V_{ph}^2} - \frac{1}{V_{c2}^2}\right)}. \quad (\text{A-7})$$

In the single-anisotropic-layer case, this becomes

$$A_5 = \frac{-A_4 V_{c2}^2}{\left(1 - \frac{V_{c2}^2}{V_{p2}^2(1 + 2\eta)}\right)}. \quad (\text{A-8})$$

If η is small, this reduces to equation (10), which may often be used more generally than the derivation implies, e.g., in the multilayer context, just as was done for P -waves by Alkhalifah and Tsvankin (1995).

Conversion-point offset

To carry out the Taylor series [equation (15)], we use the methods of Tsvankin and Thomsen (1994). Of course, the normal-incidence term C_0 yields the asymptotic conversion

point [equation (16)], whereas the slope term is given by

$$C_2 = \lim_{x/z \rightarrow 0} \left[\frac{d}{d(x/z)^2} (x_c/x) \right] \\ = \lim_{x/z \rightarrow 0} \left[\left(\frac{dp^2}{d(x/z)^2} \right) \frac{d}{dp^2} (x_c/x) \right] \quad (\text{A-9})$$

$$= \lim_{x/z \rightarrow 0} \left[\frac{p}{x/z^2} \left(\frac{dp}{dx} \right) \frac{d}{dp^2} (x_c/x) \right]. \quad (\text{A-10})$$

From equation (3),

$$\lim_{x/z \rightarrow 0} \frac{x}{p} \left(\frac{dx}{dp} \right) = \lim_{x/z \rightarrow 0} \frac{x}{p} \left(\frac{x}{p} + p \frac{d}{dp} (V_p^2 t_p + V_s^2 t_s) \right) \\ = (V_p^2 t_{p0} + V_s^2 t_{s0})^2. \quad (\text{A-11})$$

From equation (12),

$$\lim_{x/z \rightarrow 0} \frac{d}{dp^2} (x_c/x) = \frac{c_0^2}{2} \left(\frac{t_{s0}}{t_{p0}} \right) \left(\frac{V_s^2}{V_p^2} \right) (V_p^2 - V_s^2) \quad (\text{A-12})$$

Combining equations (A-9)–(A-12) yields equation (15) of the main text for the Taylor series coefficient. Then the approximation in equation (18) may be used to extend the accuracy of the expression all the way to infinite values of x/z . Since the derivation never simplifies velocity terms with time terms, we can generalize to the many-layered, polar-anisotropic case by replacing $V_p^2 \rightarrow V_{p2}^2$, etc. The corresponding expression in $(x/t_{c0} V_{c2})$, given in equation (26), is obtained from the foregoing by using the scale factor $z/t_{c0} = (\bar{V}_p/V_p)[(1 + 1/\gamma_{eff})(1 + \gamma_0)]^{-1/2}$.

Time-to-depth conversion

Given the definition of the interval C -wave velocity in equation (31), we carry out the differences indicated and find that

$$V_{ci}^2 = \frac{V_{pi}^2 \Delta t_{0pi} + V_{si}^2 \Delta t_{0si}}{\Delta t_{c0i}} \quad (\text{A-13})$$

$$= \frac{V_{pi}^2}{1 + \gamma_{0i}} + \frac{V_{si}^2}{1 + 1/\gamma_{0i}}. \quad (\text{A-14})$$

If one neglects any rapid spatial variation of velocity within the interval between the reflectors, this interval is just a homogeneous layer, and the difference between rms and arithmetic average interval velocities is also neglected. If this layer is isotropic, then equation (A-14) simplifies to equation (32). If it is anisotropic, it simplifies to equation (35).